

# Strangeness Electromagnetic Production on Nucleons and Nuclei

Petr Bydžovský\* and Miloslav Sotona

*Nuclear Physics Institute, Řež near Prague, Czech Republic*

October 31, 2018

## Abstract

Isobar models for the electromagnetic production of kaons are discussed with emphasis on the  $K^+$  photoproduction at very small kaon angles and  $K^0$  photoproduction on deuteron. Distorted-wave impuls approximation calculations of the cross sections for the electroproduction of hypernuclei are presented on the case of the  ${}_{\Lambda}^{12}\text{B}$  production.

*Key words:* Kaon, photoproduction, electroproduction, hypernucleus

*PACS:* 13.60.Le, 25.20.Lj, 25.30.Rw, 21.80.+n

## 1 Introduction

The photo- and electroproduction of kaons on nucleons and nuclei provides us with additional information about a structure and interactions of baryons. Studying the production on nucleons we learn about a reaction mechanism (quark models versus an effective Lagrangian theory with hadrons), couplings and form factors of hadrons, and look for new “missing” resonances. Moreover, we also need a correct description of the elementary production process, particularly at small kaon angles, to study the electroproduction of hypernuclei [1].

Producing a  $\Lambda$  hyperon inside ordinary nuclei allows us to probe a structure deep inside the nucleus because the  $\Lambda$ s are not Pauli blocked there. Revealing the structure of hypernuclei gives us new information about the hyperon-nucleon interactions, especially about the spin-dependent part which is not accessible by today viable experiments on the  $\Lambda$ -nucleon scattering.

A detailed study of the electromagnetic strangeness production is enabled by new ample data of good quality from various laboratories: JLab, ELSA, SPring-8, ESRF, LNS and MAMI. These data allow to perform a detailed analysis of the elementary process [2, 3]. Recent data on the photoproduction of neutral kaons off deuteron from Tohoku University [4, 5] facilitate doing more rigorous tests of models for the elementary process [5, 6].

## 2 Photo- and Electroproduction of Kaons on Nucleons

Description of the electroproduction process can be formally reduced to investigation of a binary process of the photoproduction by virtual photons since the electromagnetic coupling constant is small enough to justify the one-photon exchange approximation.

There are many approaches to treat the photoproduction process. Among them isobar models based on an effective Lagrangian description considering only hadron degrees of freedom are suitable for their further use in the more complex calculations of the electroproduction of hypernuclei. Other approaches are eligible either for higher energies ( $E_\gamma > 4$  GeV), the Regge

---

\*bydz@ujf.cas.cz

model [7], or to the threshold region, the Chiral Perturbation Theory [8]. Quark models [9] are too complicated for their further use in the hypernuclear calculations. Another approach, aimed at the forward-angle production, is the hybrid Regge-plus-resonance model [10] (RPR) in which a nonresonant part of the amplitude is generated by the  $t$ -channel Regge-trajectory exchange and a resonant behaviour is shaped by the exchanges of  $s$ -channel resonances like in isobar models.

In the effective hadron Lagrangian approach, various channels connected via the final-state interaction (meson-baryon rescattering processes) have to be treated simultaneously to take unitarity properly into account [11, 12]. In Ref. [12] the coupled-channel approach has been used to include effects of the  $\pi N$  intermediate states in the  $p(\gamma, K^+) \Lambda$  process. However, tremendous simplifications originate in neglecting the rescattering effects in the formalism assuming that they are included to some extent by means of effective values of the strong coupling constants fitted to data. This simplifying assumption was adopted in many of the isobar models, e.g., Saclay-Lyon A (SLA) [13], Kaon-MAID (KM) [14], and Janssen *et al.* [15].

In the isobar models, the amplitude obtains contributions from the Born terms and exchanges of resonances. Due to absence of a dominant resonance in the photoproduction of kaons (unlike in the  $\pi$  and  $\eta$  photoproduction) large number of various combinations of the resonances with mass below 2 GeV must be taken into account [13]. This number of models (resonance combinations) is limited considering constraints set by SU(3) [13, 14] and crossing symmetries [16, 13] and by duality hypothesis [16]. Adopting the SU(3) constraints to the two main coupling constants, however, makes the contribution of the Born terms nonphysically large [15]. To reduce this contribution, either hyperon resonances [13] or hadron form factors [14] must be added, or a combination of both [15]. Here we use especially the SLA and KM models.

Common to the KM and SLA models is that, besides the extended Born diagrams, they also include the kaon resonances  $K^*(890)$  and  $K_1(1270)$ . These models differ in a choice of  $s$ - and  $u$ -channel resonances in the intermediate state, in a treatment of the hadron structure, and in a set of experimental data to which free parameters were adjusted. However, the two main coupling constants,  $g_{KN\Lambda}$  and  $g_{KN\Sigma}$ , fulfil limits of 20% broken SU(3) symmetry [13] in both models. In the SLA model, one nucleon and four hyperon resonances are included and their coupling constants were fitted to the old data [17] and the first results of SAPHIR by Bockhorst *et al.* [18]. In the KM model, four nucleon but no hyperon resonances were assumed and parameters of the model were fitted to the old and SAPHIR [19] data. The SLA and KM models were expected to provide reasonable results for the photon energies below 2.2 GeV. In the SLA model, hadrons are treated as point-like objects, in contrast to the KM model in which phenomenological hadron form factors are inserted in the hadron vertexes [14] to stimulate a structure of hadrons. The form factors are included maintaining the gauge invariance of the amplitude [14].

## 2.1 Forward-angle $K^+ \Lambda$ Photoproduction

A good quality description of the elementary process minimises uncertainty in the calculations of excitation spectra for the hypernucleus electroproduction [1]. In Fig. 1 we compare predictions of various phenomenological models for the differential cross section with experimental data at two photon laboratory energies. For the lower energy (the left panel) the theoretical predictions reveal a good agreement with data for  $\theta_K^{c.m.} > 45^\circ$ . Results for the kaon angles smaller than  $45^\circ$  differ considerably even for the modern models SLA and KM. These models differ by  $\approx 30\%$  at  $\theta_K^{c.m.} \approx 0$ . At higher energy, 2.2 GeV (the right panel), the discrepancy of the model predictions at forward kaon angles is as large as several hundreds of per-cent.

The damping of the cross sections at very forward angles and higher energies, seen in the right panel of Fig. 1, can be understood based on analysis of the SLA and H2 [20] models. In the SLA model, the cross section at  $\theta_K^{c.m.} < 30^\circ$  is dominated by the Born terms, particularly by the electric part of the proton exchange. This contribution makes a plateau in the cross

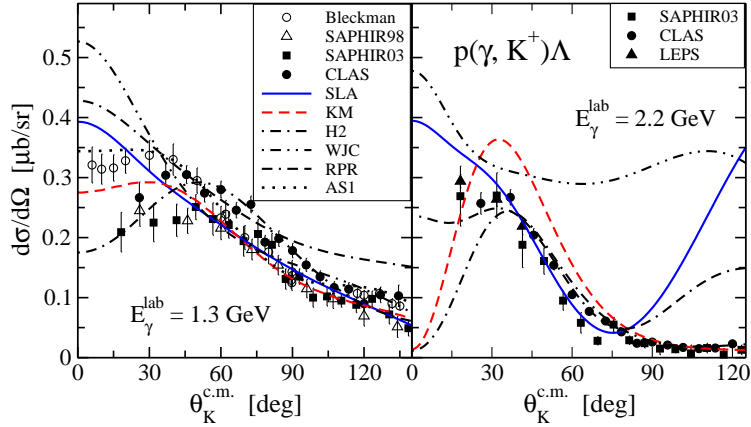


Figure 1: Predictions of the models Saclay-Lyon A [13], Kaon-MAID [14], H2 [20], Williams-Ji-Cotanch (WJC) [16], Regge-Plus-Resonance (RPR) [10], and Adelseck-Saghai (AS1) [17] are compared with data from Refs. [21] (Bleckman), [19] (SAPHIR98), [22] (SAPHIR03), [23] (CLAS), and [24] (LEPS) at two photon laboratory energies.

section as the angle goes to zero. This feature would be similar in the H2 model since values of the coupling constants,  $g_{K+\Lambda p}$  and  $g_{K+\Sigma p}$ , are almost equal to those in SLA. The situation is, however, different due to a strong suppression of the proton term caused by the hadron form factors in the H2 model, which is of the order of 0.002 in the cross section at 2 GeV. In this energy region, resonances contribute only in interference with the Born terms so that they cannot fill up the dip. This strong suppression of the Born terms in the models with the hadron form factors leads, therefore, to a pronounced dip in the differential cross section at very small angles (see Fig. 1 for the results of the H2 and KM models). Lack and mutual inconsistency of data at very small angles makes fitting of models in this kinematical region problematic [3].

This low-quality description of the elementary process in the kinematical region relevant for the hypernucleus calculations causes a large uncertainty in predictions of the cross sections for the hypernucleus production as demonstrated in Fig. 2 for the energy 1.3 GeV. Theoretical calculations of the cross sections for the electroproduction of  ${}^{12}_{\Lambda}B$  (the small momentum transfer,

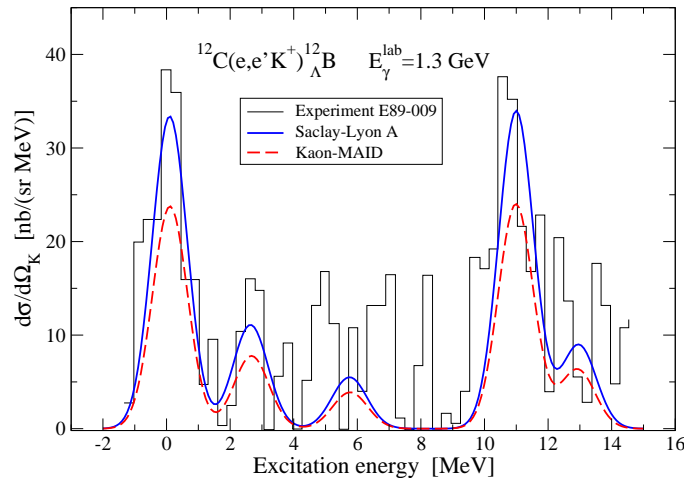


Figure 2: Results of the DWIA calculations of the cross section for the electroproduction of  ${}^{12}_{\Lambda}B$  at 1.3 GeV using the Saclay-Lyon A and Kaon-MAID models for the elementary production operator. Data are adopted from Ref. [25].

$Q^2 = -3 \cdot 10^{-6} \text{ (GeV/c)}^2$ , allows a comparison with the photoproduction cross section) are compared with the data from JLab experiment in Hall C [25]. The difference in model predictions amounts to  $\approx 30\%$  which corresponds to the difference at  $\theta_K^{\text{c.m.}} \approx 0$  seen in the left panel of Fig. 1.

### 3 Photoproduction of $K^0$ on Deuteron

The inclusive cross section for the  $d(\gamma, K^0)YN'$  or  $d(\gamma, \Lambda)KN'$  reactions (Y stands for  $\Lambda$  or  $\Sigma$  and  $N'$  for proton or neutron) in a threshold region is calculated in the impulse approximation in which the nucleon  $N'$  acts as a spectator [26]. Contributions of the final-state interaction (FSI) to the inclusive cross section were shown to be small in the studied kinematical region [27, 6]. Moreover, we assume that a part of the  $KY$  rescattering effects is absorbed in the coupling constants of the elementary amplitude and that the  $KN$  interaction is weak on the hadron scale. The main lack of precision, therefore, comes from ignoring the  $YN$  FSI. In the calculations we have chosen the *off-shell* approximation [26] in which the four-momentum is conserved in the production vertex forcing the target nucleon off its mass shell. The momentum distribution of the target nucleon is described by the nonrelativistic Bonn deuteron wave function OBEPQ [28]. More details about the calculations can be found in Ref. [26].

In the elementary amplitude, the strong coupling constants in the  $K^0\Lambda$  and  $K^+\Lambda$  channels are related via the  $SU(2)$  isospin symmetry, e.g.  $g_{K^+\Lambda p} = g_{K^0\Lambda n}$  and  $g_{K^+\Sigma^0 p} = -g_{K^0\Sigma^0 n}$ . In the electromagnetic vertexes a ratio of the neutral to charged coupling constants have to be known. For the nucleon and its resonances the ratio can be related to the known helicity amplitudes of the nucleons [29] whereas for the kaon resonances the ratio relates to the decay widths known only for the  $K^*$  meson [29]:  $r_{K^*} = -\sqrt{\Gamma_{K^{*0} \rightarrow K^0 \gamma} / \Gamma_{K^{*+} \rightarrow K^+ \gamma}} = -1.53$  where the sign was set from the quark model prediction. Since the decay widths of the  $K_1$  meson are unknown the appropriate ratio,  $r_{K_1}$ , have to be fixed in the models. It was fitted to the  $K^0\Sigma^+$  data in KM [14],  $r_{K_1} = -0.45$ , but it is a free parameter in SLA (see also Refs. [5] and [26]). For hyperons, the electromagnetic vertex is not changed in the  $K^0\Lambda$  channel.

In Figure 3 results for the momentum spectra of the  $d(\gamma, K^0)\Lambda p$  reaction calculated with different elementary amplitudes are shown in comparison with recent data on the  $d(\gamma, K^0)YN'$  reaction [5]. Contributions of the  $\Sigma$  channels are very small in the low-energy region (Fig. 3a) and at the spectator-kinematics region, the main peak in Fig. 3b [5]. The KM model do not describe

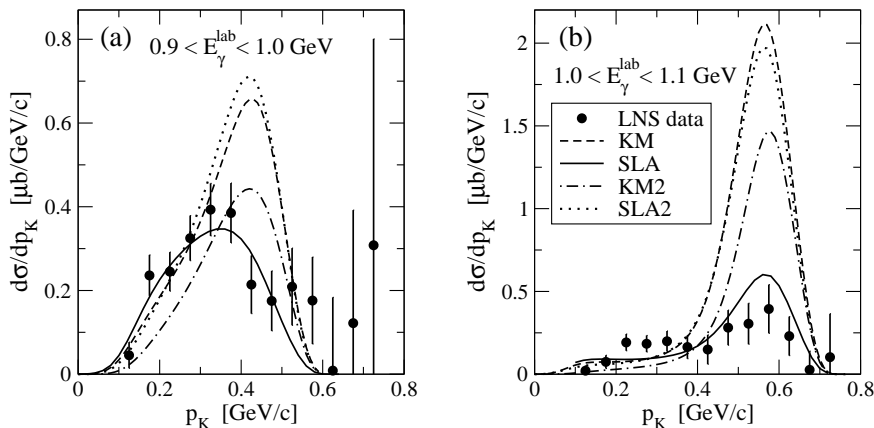


Figure 3: Inclusive energy-averaged, (a)  $0.9 < E < 1.0$  GeV and (b)  $1.0 < E < 1.1$  GeV, and kaon-angle-integrated,  $0.9 < \cos(\theta_K) < 1.0$ , momentum spectra for the  $d(\gamma, K^0)YN'$  reaction. Calculations with the  $\Lambda p$  in the final state using various elementary amplitudes are compared with data from Ref. [5].

the data well, especially at the spectator-kinematics region (dashed line). Results of KM cannot be improved even if the  $r_{K1}$  parameter is refitted to the low-energy data (Fig. 3a):  $\chi_{\text{n.d.f.}}^2 = 3.64$  with  $r_{K1} = -2.34$ . Results of this fit are displayed as KM2 (dashed-dotted line) in Fig. 3. It is seen that the KM model cannot fit a proper shape of the momentum spectra.

The SLA model with  $r_{K1} = -2.09$ , fitted to the low-energy data ( $\chi_{\text{n.d.f.}}^2 = 0.88$ ) [5], gives good results in both energy regions. To demonstrate a flexibility of this model we show results of the model with  $r_{K1} = -3.4$  denoted SLA2. This version of the Saclay-Lyon model gives very similar values of the cross sections for the  $n(\gamma, K^0)\Lambda$  process as the KM model and therefore its results for the  $d(\gamma, K^0)\Lambda p$  reaction are close to those of the KM model (Fig. 3). This demonstrates that results of the SLA model in the  $K^0 p$  channel are very sensitive to the ratio of the decay widths of the  $K_1$  resonance ( $r_{K1}$ ).

The angular dependence of the elementary cross sections differs for the models KM and SLA. The latter gives the cross sections enhanced at the backward hemisphere whereas the KM model reveal a more complex resonance pattern dominated by the  $N^*(1720)$  resonance [5, 26]. In general, the elementary models which possess the backward-peaked cross sections, e.g. SLA, give much better results for the  $d(\gamma, K^0)\Lambda p$  inclusive cross sections than those with other angular dependence [5], e.g. KM and SLA2 in Fig. 3. This comparison shows that the Tohoku data prefer models which predict the cross section for the  $n(\gamma, K^0)\Lambda$  process enhanced at the backward hemisphere.

Predictions of the momentum distributions in the  $d(\gamma, \Lambda)KN'$  reaction are shown in Fig. 4. Results for the energy averaged and  $\Lambda$ -angle integrated inclusive cross sections are plotted for the  $K^0 p$  and  $K^+ n$  channels using the SLA and KM models. Predictions of the models agree each other for the  $K^+ n$  channel except for the low-energy and small-angle region (Fig. 4a). In the kinematical regions of Figs. 4b, c, and d, the full results ( $K^+ n + K^0 p$ ) of the models differ enough to allow a new data to discriminate between the models.

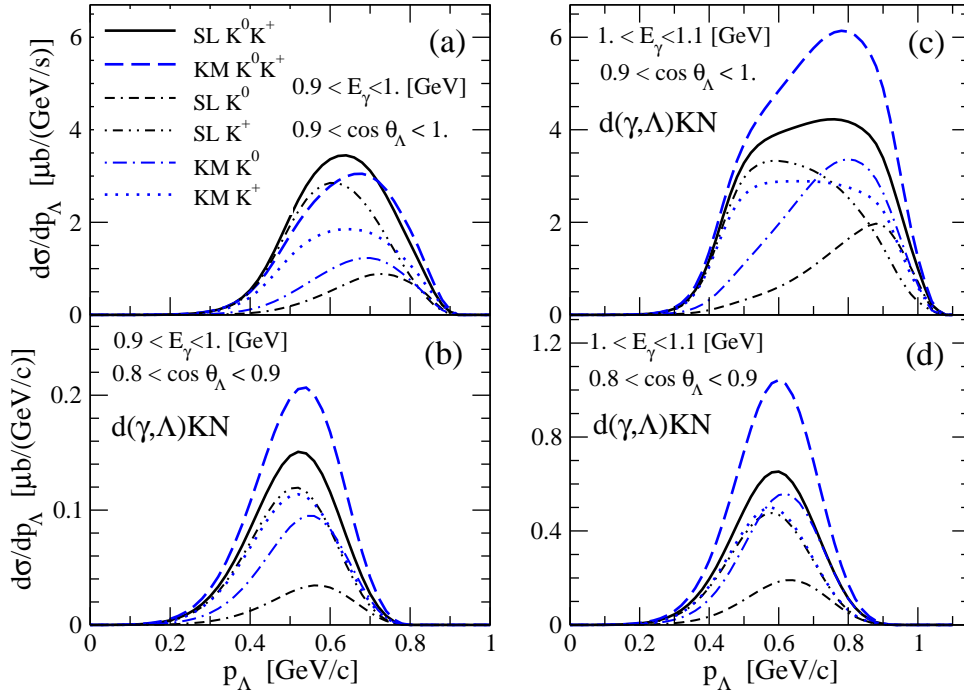


Figure 4: Predictions of inclusive energy-averaged and  $\Lambda$ -angle-integrated momentum spectra for the  $d(\gamma, \Lambda)KN'$  reaction. Results of the SLA and KM models are shown for various final states.

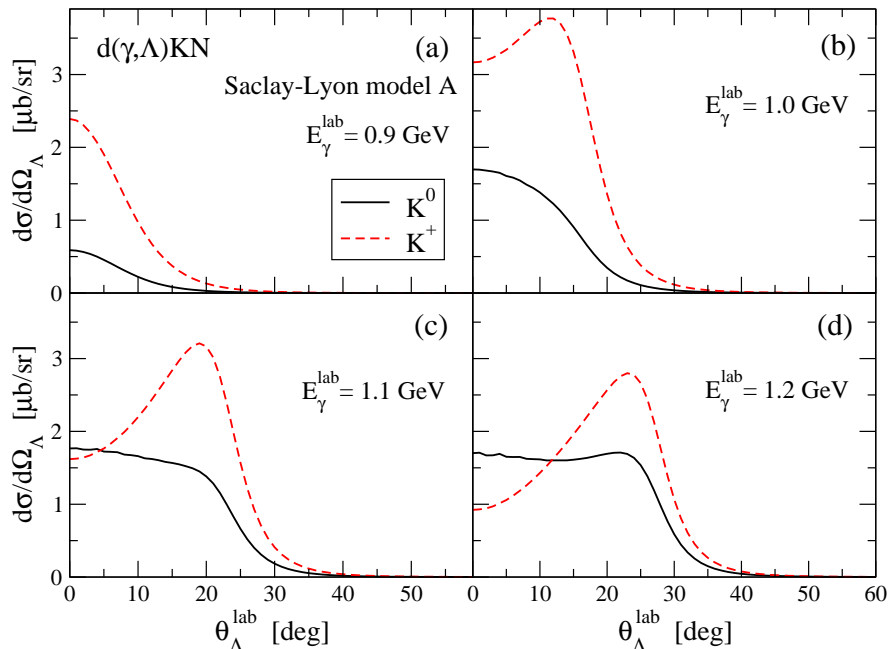


Figure 5: Predictions of the  $\Lambda$ -momentum-integrated cross sections as a function of  $\Lambda$  laboratory angle. Calculations in PWIA using the Saclay-Lyon A model with  $r_{K1} = -2.09$  are shown for  $K^0$  and  $K^+$  in the final state.

In Figure 5 the inclusive differential cross section is plotted in dependence on the  $\Lambda$  angle. Results show that the cross sections for the  $K^+n$  and  $K^0p$  channels are centred at  $\Lambda$  angles smaller than  $\approx 30^\circ$  for photon energies below 1.1 GeV. This indicates a possibility to measure the total cross section of the reaction if an acceptance of the detector can cover this small-angle region. The reaction with the  $K^+n$  final state reveals different angular dependence than that with the  $K^0p$  state, being peaked at  $20^\circ$  for energy larger than 1 GeV (see Figs. 5b, c, and d).

## 4 Electroproduction of p-shell Hypernuclei

The cross sections for the electroproduction of hypernuclei are calculated in the framework of the distorted-wave impulse approximation (DWIA) [30]. The ingredients of the many-body matrix element in the DWIA are nonrelativistic nuclear and hypernuclear wave functions, an operator for the elementary-production process, an incoming virtual-photon wave function (in the one-photon exchange approximation), and an outgoing kaon distorted wave function. The calculations are performed in the laboratory frame neglecting the Fermi motion. For the elementary operator we use an isobar model, e.g. the Saclay-Lyon model discussed in Sect. 2. The kaon distorted wave is calculated in the optical-potential model assuming the eikonal approximation [30].

The nuclear wave functions are obtained in the shell-model calculations with an effective p-shell interaction. The in-medium  $\Lambda N$  interaction used in the shell-model calculations of the hypernucleus wave functions is fitted to precise  $\gamma$ -ray spectra of p-shell nuclei [31].

In the right part of Fig. 6 we show low-energy excitation levels of the  ${}^{12}_{\Lambda}\text{B}$  build up on levels of the core nucleus  ${}^{11}\text{B}$  (the left part) assuming the weak coupling scheme. The low-energy states in the spectrum of  ${}^{12}_{\Lambda}\text{B}$  (doublets) are generated by coupling of the  $\Lambda$  in  $s$ -state to the lowest negative-parity states in  ${}^{11}\text{B}$ . The higher-energy multiplets in  ${}^{12}_{\Lambda}\text{B}$  are formed by coupling of the  $p_{1/2}$  or  $p_{3/2}$   $\Lambda$ 's to the lowest negative-parity states of  ${}^{11}\text{B}$ . The dashed line in Fig. 6 indicates the energy of the quasi-free production reaction.

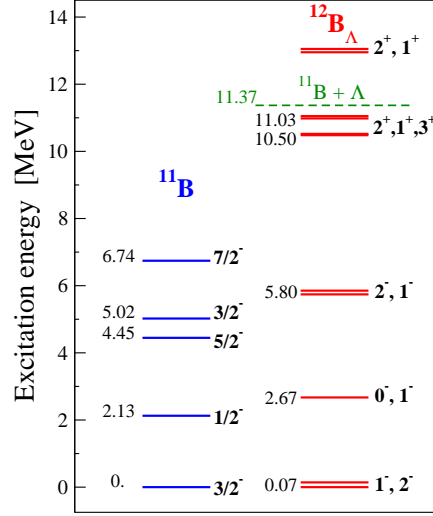


Figure 6: Schemes of the low-lying energy levels for the core nucleus  $^{11}\text{B}$  (left) and hypernucleus  $^{12}_{\Lambda}\text{B}$  (right). The dashed line indicates the threshold for the  $\Lambda$  emission. The energies are in MeV.

Results of the DWIA calculations using the SLA model for the electroproduction of  $^{12}_{\Lambda}\text{B}$  are compared in Fig. 7 with JLab data from Hall A [32]. The cross sections for members of the multiplets are indicated by bars. Agreement of the calculations with data is good for the part of the spectra where the  $\Lambda$  is in  $s$ -state (the first three peaks). The region of  $p_{\Lambda}$  states (the 2nd main peak), especially the strengths on both sides of the 2nd main peak, is not well described using these simple shell-model wave functions. More complex calculations have to be performed, e.g. assuming  $1h\omega$  excitations, to better understand the  $p_{\Lambda}$  region. Similar conclusions were also drawn for the  $^{16}\text{O}(e,e'\text{K}^+)^{16}_{\Lambda}\text{N}$  reaction [33]. The reasonable values of the cross sections provided by the DWIA calculations with the SLA model suggest that the Saclay-Lyon model gives also good values of the elementary cross section at very forward kaon angles.

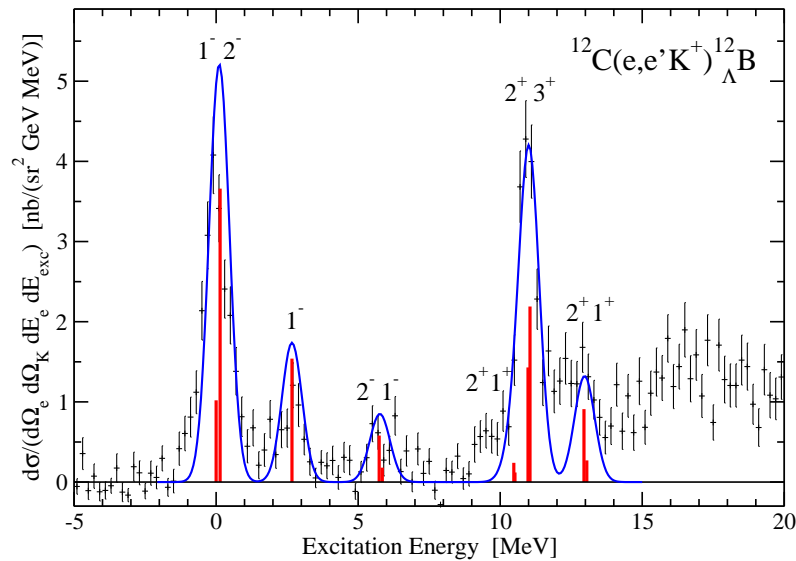


Figure 7: Excitation-energy spectrum of  $^{12}_{\Lambda}\text{B}$  at  $E_{\gamma}^{\text{lab}} = 2.2$  GeV calculated in DWIA using the SLA model. The overall prediction (solid line) and the cross sections for particular states (bars) are compared with data from Ref. [32].

## 5 Summary

Data at very small kaon angles are needed to fix the models for the  $K^+$  photoproduction at forward angles which is necessary for reliable hypernuclear calculations. The data on the  $K^0$  photoproduction off deuteron near threshold prefer the models which give enhancement of the cross section at the backward kaon angles. Predictions of the DWIA shell-model calculations agree well with the spectra of  ${}^{12}_{\Lambda}\text{B}$  and  ${}^{16}_{\Lambda}\text{N}$  for the  $\Lambda$  in  $s$ -state. In the  $p_{\Lambda}$  region, more elaborate calculations, e.g. taking into account core-nucleus  $1h\omega$  states, are needed to fully understand the new data. The Sacaly-Lyon model of the elementary process gives reasonable cross sections for the hypernucleus production which suggests that this model describes correctly the elementary process at forward kaon angles.

One of the authors (P.B.) wishes to thank the organisers for their kind invitation to this highly stimulating Conference. This work was supported by the Grant Agency of the Czech Republic, grant 202/08/0984.

## References

- [1] P. Bydžovský, M. Sotona, T. Motoba, K. Itonaga, K. Ogawa, and O. Hashimoto, arXiv:0706.3836 [nucl-th].
- [2] T. Mart and A. Sulaksono, Phys. Rev. C **74** (2006) 055203.
- [3] P. Bydžovský and T. Mart, Phys. Rev. C **76** (2007) 065202; arXiv:nucl-th/0605014.
- [4] T. Watanabe *et al.*, Phys. Lett. B **651** (2007) 269; arXiv:nucl-ex/0607022.
- [5] K. Tsukada *et al.*, Phys. Rev. C **78** (2008) 014001.
- [6] A. Salam, T. Mart, and K. Miyagawa, Mod. Phys. Lett. A **24** (2009) 968; arXiv:0906.0316 [nucl-th].
- [7] M. Guidal, J.-M. Laget, M. Vanderhaeghen, Nucl. Phys. A **627** (1997) 645.
- [8] S. Steininger and U.-G. Meissner, Phys. Lett. B **391** (1997) 446.
- [9] B. Saghai, in *Proc. of Electrophotoproduction of Strangeness on Nucleons and Nuclei*, Sendai, Japan, 16-18 June, 2003, (Eds. K.Maeda, H.Tamura, S.N.Nakamura, and O.Hashimoto). World Sci., 2004, p.53; nucl-th/0310025.
- [10] T. Corthals, J. Ryckebusch, and T. Van Cauteren, Phys. Rev. C **73** (2006) 045207; T. Corthals, T. Van Cauteren, P. Van Craeyveld, J. Ryckebusch, and D.G. Ireland, Phys. Lett. B **656** (2007) 186.
- [11] G. Penner and U. Mosel, Phys. Rev. C **66** (2002) 055212; A. Usov and O. Scholten, Phys. Rev. C **72** (2005) 025205.
- [12] W.T. Chiang, F. Tabakin, T.-S.H. Lee, B. Saghai, Phys. Lett. B **517** (2001) 101.
- [13] J.C. David, C. Fayard, G.-H. Lamot, B. Saghai, Phys. Rev. C **53** (1996) 2613; T. Mizutani, C. Fayard, G.-H. Lamot, B. Saghai, Phys. Rev. C **58** (1998) 75.
- [14] T. Mart and C. Bennhold, Phys. Rev. C **61** (1999) 012201(R); T. Mart, Phys. Rev. C **62** (2000) 038201; C. Bennhold, H. Haberzettl and T. Mart, arXiv:nucl-th/9909022; T. Mart, C. Bennhold, H. Haberzettl, and L. Tiator, <http://www.kph.uni-mainz.de/MAID/kaon/kaonmaid.html>.

- [15] S. Janssen, J. Ryckebusch, D. Debruyne, and T. Van Cauteren, Phys. Rev. C **65** (2001) 015201.
- [16] R.A.Williams, Chueng-Ryong Ji, S.R.Cotanch, Phys. Rev. C **46** (1992) 1617.
- [17] R.A. Adelseck and B. Saghai, Phys. Rev. C **42** (1990) 108.
- [18] M. Bockhorst *et al.*, Z. Phys. C **63** (1994) 37.
- [19] M.Q. Tran *et al.*, Phys. Lett. B **445** (1998) 20.
- [20] P. Bydžovský and M. Sotona, Nucl. Phys. A **754** (2005) 243c; nucl-th/0408039.
- [21] A. Bleckmann *et al.*, Z. Phys. **239** (1970) 1.
- [22] K.-H. Glander *et al.*, Eur. Phys. J. A **19** (2004) 251; nucl-ex/0308025.
- [23] R. Bradford *et al.*, Phys. Rev. C **73** (2006) 035202; nucl-ex/0509033.
- [24] M. Sumihama *et al.*, Phys. Rev. C **73** (2006) 035214.
- [25] T. Miyoshi *et al.*, Phys. Rev. Lett. **90** (2003) 232502.
- [26] P. Bydžovský, M. Sotona, O. Hashimoto, and T. Takahashi, nucl-th/0412035.
- [27] A. Salam, K. Miyagawa, T. Mart, C. Bennhold and W. Glöckle, Phys. Rev. C **74** (2006) 044004.
- [28] R. Machleidt, K. Holinde, and Ch. Elster, Phys. Rep. **149** (1987) 1.
- [29] C. Amsler *et al.* (Particle Data Group), Phys. Lett. B **667** (2008) 1.
- [30] M. Sotona and S. Frullani, Prog. Theor. Phys. Suppl. **117** (1994) 151.
- [31] D.J. Millener, Springer Lecture Notes Phys. **724** (2007) 31.
- [32] M. Iodice *et al.*, Phys. Rev. Lett. **99** (2007) 052501.
- [33] F. Cusanno *et al.*, Phys. Rev. Lett. **103** (2009) 202501.